おわりに

ChIP-seq解析では，標的タンパク質の種類によりサンプルの調製方法や情報解析の手法が異なる．このように，すべてのChIP-seq実験に適用できる統一的な実験プロトコルが存在しないことが，データの品質のばらつきを生み出す一因となっているように見える．近年の大規模データを扱った研究論文は，実験方法の記述が簡略化される傾向があるが，基本に立ち返り，再現性を検証できるように情報を提供するべきである．ENCODEのガイドラインは，今後，ChIP-seq解析論文を投稿する際のスタンダードとなるかもしれない．

文献

1） Park, P. J. : Nature Rev. Genet., 10 : 669-680, 2009
2） International Human Genome Sequencing Consortium : Nature, 431 : 931-945, 2004
3） The ENCODE Project Consortium : Science, 306 : 636-640, 2004
4） Djebali, S. et al. : Nature, 489 : 101-108, 2012
5） The ENCODE Project Consortium : Nature, 447 : 799-816, 2007
6） The ENCODE Project Consortium : Nature, 489 : 57-74, 2012
7） The ENCODE Project Consortium : PLoS Biol, 9 : e1001046, 2012
8） Rosenbloom, K. R. et al. : Nucleic Acids Res., 40 : D912-D917, 2012
9） Chen, Y. et al. : Nat. Methods, 9 : 609-614, 2012
10） Rhee, H. S. & Pugh, F. : Cell, 147 : 1408-1419, 2011
11） Rhee, H. S. & Pugh, F. : Nature, 483 : 295-301, 2012
12） Landt, S. G. et al. : Genome Res., 22 : 1813-1831, 2012
13） Pauler, F. M. et al. : Genome Res., 19 : 221-233, 2009
14） Li, Q. et al. : Ann. Appl. Stat., 5 : 1752-1779, 2011

<著者プロフィール>
舟山　亮：2007年，東京工業大学大学院生命理工学研究科博士後期課程修了．理学博士．京都大学大学院生命科学研究科博士研究員，同科特任助教を経て，'07年10月より現所属（助教）．次世代シークエンサーを利用した解析のサポートをしながら，がん細胞のエピゲノムと遺伝子発現制御機構に興味をもって研究している．
E-mail：rfunayam@med.tohoku.ac.jp

10228–10239 *Nucleic Acids Research, 2012, Vol. 40, No. 20* *Published online 10 September 2012*
doi:10.1093/nar/gks827

Nrf2–MafG heterodimers contribute globally to antioxidant and metabolic networks

Yosuke Hirotsu[1], Fumiki Katsuoka[2,*], Ryo Funayama[3], Takeshi Nagashima[3], Yuichiro Nishida[3], Keiko Nakayama[3], James Douglas Engel[4] and Masayuki Yamamoto[1,2,*]

[1]Department of Medical Biochemistry, [2]Department of Integrative Genomics, Tohoku Medical Megabank Organization, [3]Division of Cell Proliferation, Tohoku University Graduate School of Medicine, Sendai, 980-8575, Japan and [4]Department of Cell and Developmental Biology, University of Michigan Medical School, Ann Arbor, MI 48109-220, USA

Received July 4, 2012; Revised August 6, 2012; Accepted August 9, 2012

ABSTRACT

NF-E2-related factor 2 (Nrf2) is a key transcription factor that is critical for cellular defense against oxidative and xenobiotic insults. Nrf2 heterodimerizes with small Maf (sMaf) proteins and binds to antioxidant response elements (AREs) to activate a battery of cytoprotective genes. However, it remains unclear to what extent the Nrf2–sMaf heterodimers contribute to ARE-dependent gene regulation on a genome-wide scale. We performed chromatin immunoprecipitation coupled with high-throughput sequencing and identified the binding sites of Nrf2 and MafG throughout the genome. Compared to sites occupied by Nrf2 alone, many sites co-occupied by Nrf2 and MafG exhibit high enrichment and are located in species-conserved genomic regions. The ARE motifs were significantly enriched among the recovered Nrf2–MafG-binding sites but not among the Nrf2-binding sites that did not display MafG binding. The majority of the Nrf2-regulated cytoprotective genes were found in the vicinity of Nrf2–MafG-binding sites. Additionally, sequences that regulate glucose metabolism and several amino acid transporters were identified as Nrf2–MafG target genes, suggesting diverse roles for the Nrf2–MafG heterodimer in stress response. These data clearly support the notion that Nrf2–sMaf heterodimers are complexes that regulate batteries of genes involved in various aspects of cytoprotective and metabolic functions through associated AREs.

INTRODUCTION

Defense systems against oxidative and xenobiotic stresses are conserved across species. To adapt to or resist the stresses, cells activate a multi-layered defense system tightly associated with various cellular processes. One of the most important components of such an integrated system is transcriptional regulation. In fact, many transcription factors have been identified that regulate cytoprotective genes. In vertebrates, Nrf2 (NF-E2-related factor 2) is regarded as a central regulator of antioxidant and detoxification enzyme genes.

Nrf2 is a member of the Cap'n'collar (CNC) family, a subfamily of basic region–leucine zipper (bZIP) transcription factors (1,2). Under static conditions, Nrf2 proteins are ubiquitinated by Keap1 (Kelch-like ECH-associated protein1)–Cul3 E3 ligase complex and degraded by the proteasome system (3–6). In response to stresses, Nrf2 proteins accumulate in the nucleus and activate a battery of cytoprotective genes (3). These findings are supported by data that show that *Nrf2* knockout mice are susceptible to various stresses due to the impaired activation of cytoprotective genes (7–9). Interestingly, an evolutionarily distant CNC homolog, SKN-1, also regulates a battery of cytoprotective genes in the nematode (10,11). However, the DNA-binding modality of Nrf2 and other CNC proteins is completely different from that of SKN-1 (10,12). Whereas SKN-1 functions as a monomer, Nrf2 acts as a heterodimer with a member of the small Maf (sMaf) protein family, another subfamily of bZIP transcription factors (7).

The sMaf protein family consists of functionally redundant members in mammals: MafF, MafG and MafK (13,14). Nrf2–sMaf heterodimers bind to the antioxidant response element (ARE)/electrophile responsive element

*To whom correspondence should be addressed. Tel: +81 22 717 8084; Fax: +81 22 717 8090; Email: masiyamamoto@med.tohoku.ac.jp
Correspondence may also be addressed to Fumiki Katsuoka. Tel: +81 22 717 8089; Fax: +81 22 717 8090; Email: kfumiki@med.tohoku.ac.jp

that has been found in the regulatory regions of many cytoprotective genes (7). Whereas the ARE sequence was originally defined as RGTGACNNNGC, the core ARE sequence (TGACNNNGC) has become more widely recognized (15–17). sMaf proteins can form homodimers with themselves and bind to the Maf recognition element (MARE; TGCTGACTCAGCA). Since sMaf proteins lack a canonical activation domain, their homodimers are regarded as negative regulators (18). It has been suggested that sMaf homodimers compete with Nrf2–sMaf heterodimers for binding to the ARE embedded in the MARE (19). Other transcription factor complexes are also reported to bind to the ARE. The core ARE often bears an internal TRE (TGACTCA), leaving the possibility that AP-1 complexes, such as the Jun–Fos heterodimer, bind to the ARE or MARE (20). Furthermore, Nrf2 was able to heterodimerize with other bZIP factors including Jun, Fos and ATF4 and bind to the ARE (21,22). However, other than Nrf2–sMaf heterodimers, the contribution of these other complexes to ARE-dependent gene regulation is unclear.

The functional significance of Nrf2–sMaf heterodimers on ARE-dependent gene regulation has been investigated *in vitro* and *in vivo*. Biochemical analyses have clearly demonstrated that Nrf2 requires heterodimerization with sMaf proteins for efficient binding to DNA (23,24). A comprehensive binding motif analysis revealed that Nrf2–sMaf heterodimers require a GC sequence (or GC box) on the 3′-side of the ARE for their binding (indicated by underline; TGACNNNGC) (24). Supporting this observation, structural studies have demonstrated that sMaf proteins possess a domain called the extended homology region that recognizes the GC box (25). Genetic studies also demonstrated that the stress-inducible expression of various Nrf2 target genes was severely compromised in mouse embryonic fibroblasts that lack all three sMaf proteins (26). These studies strongly support the notion that Nrf2 requires sMaf proteins for activating ARE-dependent genes. However, it is unclear to what extent the Nrf2–sMaf heterodimer model can be applied on the genome-wide scale. In addition, a picture of a presumptive gene regulatory network that might be controlled by Nrf2–sMaf heterodimers has not been previously explored.

In this study, we performed chromatin immunoprecipitation coupled with high-throughput sequencing (ChIP-seq) to identify the genomic binding sites of Nrf2 and MafG. Compared to sites that are occupied by Nrf2 alone, many sites co-occupied by Nrf2 and MafG were shown to be highly enriched and located in genomic regions that are conserved among vertebrate species. The ARE motif was, as anticipated, significantly enriched in the Nrf2–MafG-binding sites but not in the Nrf2-alone binding sites. In addition to genes directly related to antioxidant and detoxifying enzymes, numerous genes involved in glucose metabolism and amino acid transport were also identified as inducible Nrf2–MafG target genes. Thus, these data demonstrate that Nrf2–sMaf heterodimers regulate genomic batteries of genes involved in both cytoprotective as well as specific metabolic functions through AREs.

MATERIALS AND METHODS

Cell culture

The mouse hepatoma cell line Hepa1c1c7 (Hepa1) was cultured in Dulbecco's modified Eagle's medium (Wako) supplemented with 10% fetal bovine serum and 1% penicillin–streptomycin (Gibco). Mouse embryonic fibroblasts (MEFs) from sMaf triple knockout mice (*MafF*$^{-/-}$:*MafG*$^{-/-}$:*MafK*$^{-/-}$; *F0G0K0*) and control mice (*MafF*$^{-/-}$:*MafG*$^{+/+}$:*MafK*$^{-/-}$; *F0G2K0*) were used as previously described (26).

RNA purification and quantitative PCR analysis

Total RNA was extracted using the ISOGEN RNA extraction kit (Nippon Gene) and reverse transcribed to cDNA using Super-script III (Invitrogen). The quantitative PCR (qPCR) was performed with PCR Master Mix using TaqMan probe or SYBR Green and the ABI 7300 system (Applied Biosystems). The primers and probes for the NAD(P)H:quinone oxidoreductase (*Nqo1*) detection were described previously (26). The sequences for the other primers used are provided in Supplementary Table S1. The expression levels were normalized to those of hypoxanthine–guanine phosphoribosyl transferase.

ChIP and ChIP-seq analysis

The ChIP analysis was performed as described previously (27), with minor modifications. Briefly, the cells were treated with 100 μM of diethyl maleate (DEM) for 4 h and fixed with 1% formaldehyde for 10 min at room temperature and subsequently quenched with 0.125-M glycine. The fixed samples were lysed and sonicated. The antibody incubations were performed overnight at 4°C. The cross-linking was reversed overnight at 65°C. The purified DNA was analyzed by qPCR. The antibodies used were anti-Nrf2 (Santa Cruz; sc-13032), anti-MafG (18), anti-CBP (Santa Cruz; sc-369X), anti-H3Ac (Millipore), anti-H4Ac (Millipore), anti-H3K9Ac (Upstate) and normal rabbit IgG (Santa Cruz sc-2027). The values obtained from the immunoprecipitated samples were normalized to the input DNA. The sequences for the primers used are shown in Supplementary Table S1 in the supporting materials. For the ChIP-seq analysis, the ChIP-seq libraries were prepared from 10 ng each of ChIP and input samples (quantified by Invitrogen Qubit Fluorometer) using SOLiD Fragment Library Construction Kit with SizeSelect Gels, according to the manufacturer's instructions (Life Technologies). The libraries were clonally amplified on SOLiD P1 DNA Beads by emulsion PCR and sequenced using SOLiD4 System to generate 50 base-single reads (Life Technologies). The sequenced reads were mapped to the mouse genome (mm9) using BioScope MapData. The peaks were called in the aligned sequence data using a model-based analysis of ChIP-seq (MACS) (28) and compared with input DNA that was sequenced, sonicated and amplified with a *P*-value cutoff of 10^{-5} and default values for other parameters.

Motif analysis, conservation plot and genomic distributions of binding sites

De novo DNA motif analysis and construction from ChIP-seq data were performed using MEME–ChIP (29). Conservation analysis was performed by Cistrome analysis pipeline (http://cistrome.dfci.harvard.edu/ap/) using a 300-bp window and the average vertebrate PhastCons metric (30,31). The genomic distributions of binding sites were analyzed using the *cis*-regulatory element annotation system (32).

Microarray analysis

Two independent RNA samples from Hepa1 cells treated with 100-μM DEM or vehicle for 6 h were used for the microarray analyses. The Agilent 4 × 44 K Whole-Mouse Genome Oligo Microarray slides were hybridized, washed and scanned on an Agilent Microarray Scanner according to the Agilent protocol. The expression data were subjected to statistical analysis using GeneSpring software (Silicon Genetics, Redwood City, CA, USA). The gene expression data are available through the Gene Expression Omnibus database (GEO; accession no. GSE38350).

Small interference RNA

Hepa1 cells were transfected with validated Stealth small interference RNA (siRNA) targeting Nrf2 in parallel with corresponding Stealth siRNA controls (Invitrogen) using Lipofectamine 2000 (Invitrogen), according to the manufacturer's instructions, 24 h before DEM treatment.

Immunoblot analysis

The nuclear lysates were prepared as described (33). The lysates were separated by SDS–PAGE and transferred onto Immobilon membranes (Millipore). Immunoblot analysis was carried out using anti-Nrf2 (Santa Cruz; sc-13032) and anti-Lamin B antibodies (Santa Cruz). A horseradish peroxidase-conjugated secondary antibody (Zymed) was used. Signals were detected with ECL (Enhanced Chemiluminescence) western blotting detection reagents (Amersham).

RESULTS

Genome-wide mapping of Nrf2- and MafG-binding sites

To examine Nrf2–MafG heterodimer-mediated gene regulation on a whole-genome scale, we conducted ChIP-seq analyses of the mouse hepatoma cell line, Hepa1. To activate Nrf2, we treated Hepa1 cells with the Nrf2 inducer DEM and confirmed nuclear accumulation of Nrf2 proteins [~110 kDa; (34)] by immunoblotting (Figure 1A). Then, ChIP DNA samples were prepared using specific antibodies for Nrf2 and MafG, and ChIP-seq libraries were constructed from these DNA samples as well as control input DNA samples. After confirming that the regulatory regions of well-known Nrf2 target genes, *Nqo1* and heme oxygenase-1 (*Hmox1*), were enriched in the libraries (Figure 1B), deep sequencing was performed on each of the ChIP (and control) samples. As a result, 15 534 sites for Nrf2 and 19 362 sites for MafG were identified as significantly enriched in each library (Figure 1C). Among these, 3265 sites were identified as Nrf2–MafG co-occupied sites (Figure 1C), including the previously identified regulatory regions of *Nqo1* and *Hmox1* (Figure 1D).

Then, we examined the location of the enriched sites relative to the annotated gene structures. Overall, the sites occupied by Nrf2 or MafG alone as well as the sites co-occupied by Nrf2–MafG were predominantly located in the intergenic regions (Figure 1E). However, the Nrf2–MafG co-occupied sites were slightly more enriched in the proximal and distal promoter regions (Figure 1E) suggesting their participation in promoter (rather than enhancer or silencer) processes.

We next focused on the sites located within 10 kb of the transcription start sites (TSS), where many functional regulatory regions are located. In these regions, there are 1638 and 3045 sites occupied by Nrf2 or MafG alone, respectively, and there are 702 sites co-occupied by Nrf2 and MafG (Figure 2A). To elucidate the possible functional significance of Nrf2–MafG heterodimer-mediated gene regulation, we investigated in detail the sites occupied by the Nrf2–MafG heterodimer as compared to those occupied by Nrf2 alone (details of the sites occupied by MafG alone will be published elsewhere). According to the UCSC PhastCons conservation scores (see 'Materials and Methods' section), the center of the Nrf2–MafG-binding sites was more highly conserved among vertebrate species compared with that of the Nrf2 single binding sites (Figure 2B), suggesting functional significance of the Nrf2–MafG-binding sites.

The profile plot showed that the average enrichment of Nrf2 was much greater at the Nrf2–MafG-binding sites than at the Nrf2 single binding sites (Figure 2C). In fact, the Nrf2–MafG-binding sites were largely composed of sites with high ChIP enrichment, whereas most of the Nrf2 single binding sites were composed of sites with only low enrichment (Figure 2D). Taken together, these observations suggest that sites co-occupied by Nrf2 and MafG serve as high affinity sites that allow stable binding and might be critical for Nrf2–sMaf-mediated gene regulation.

The ARE motif is highly enriched in the sites co-occupied by Nrf2 and MafG

To determine whether the ARE motif is enriched in the sites identified by ChIP-seq, we performed *de novo* motif analysis. The ARE motif was determined to be enriched in the Nrf2–MafG-binding sites (E-value = 5.0×10^{-437}, Figure 3A and B). Interestingly, the nucleotide immediately 5′ to the enriched ARE motif tended to be A or G (Figure 3B, N3 position), which is reported to be an unfavorable nucleotide for MafG homodimer binding (24). Therefore, we suggest (without further experimental support here) that the majority of the enriched AREs do not effectively recruit sMaf homodimers. The MARE-like motif, which possesses bilateral GC boxes, was enriched in the MafG single binding sites

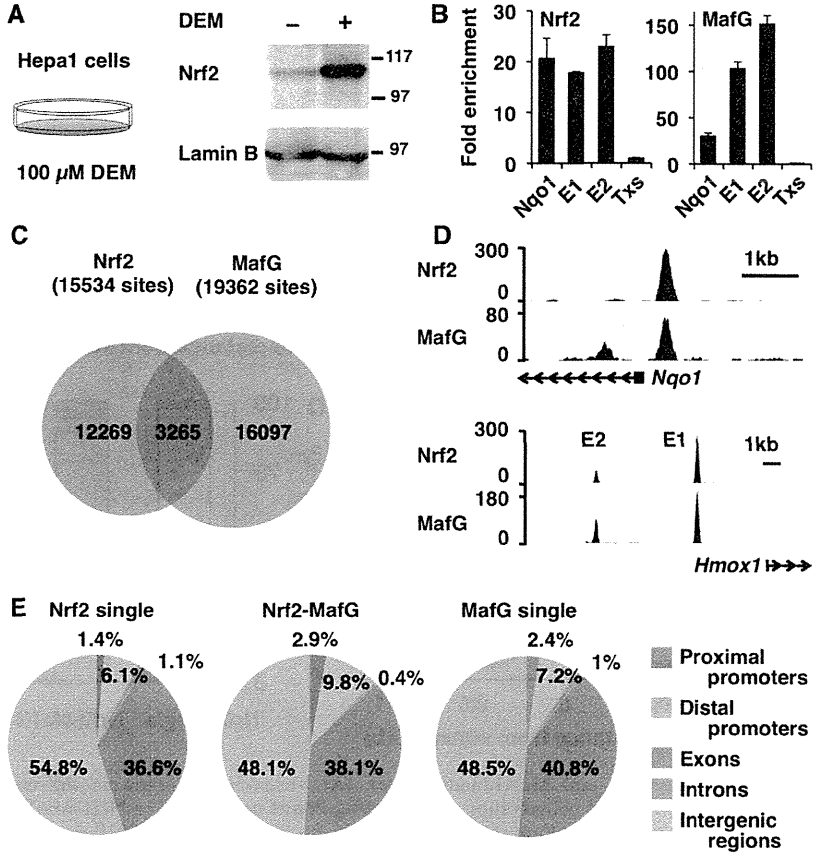

Figure 1. Identification of Nrf2- and MafG-binding sites by ChIP-seq analysis. (**A**) Immunoblot analysis of Nrf2 protein in nuclear lysates of Hepa1 cells treated with 100-μM DEM or DMSO for 4 h. Lamin B was detected as a loading control. The molecular weight in kDa is shown at right. (**B**) Validation of the ChIP-seq library. ChIP was performed with Nrf2 and MafG antibodies, and the precipitated DNA was used to make the ChIP-seq library. qPCR was performed to verify the enrichment of regulatory regions of the *Nqo1* gene and *Hmox-1* gene E1 and E2 enhancers. The third intron of the thromboxane synthase (*Txs*) gene was used as a negative control locus, and its level was set to 1. (**C**) Venn diagram showing the overlap between the Nrf2 and MafG-binding sites. Overlapping peaks are defined by an intersection of the distance between the peak summit within 268 bp. (**D**) The ChIP-seq profiles around the *Nqo1* promoter and *Hmox-1* E1 and E2 enhancers are shown as UCSC genome browser shots. (**E**) Identification of the genomic location of Nrf2 single binding sites, Nrf2–MafG-binding sites and MafG single binding sites using CEAS. The diagram illustrates the overall distribution of the Nrf2–MafG-binding sites into the proximal promoters (<−1 kb), distal promoters (−1 to −10 kb), exons, introns and intergenic regions.

(*E*-value = 7.3×10^{-106}, Figure 3C), suggesting that sMaf homodimers bind to these sites. By contrast, neither the ARE motif nor the MARE motif was significantly enriched in the Nrf2 single binding sites (data not shown). Taken together with previous *in vitro* analyses, the present genomic analyses of culture cells suggest that Nrf2–sMaf heterodimers are the predominant complexes that bind to AREs.

An enriched ARE motif internalizes an ideal sMaf-binding motif

Whereas the core ARE motif has been defined as TGACNNNGC, where N is a variable nucleotide (Figure 3A, N8, N9 and N10 positions, hereafter designated N8–10), the majority of enriched AREs in the Nrf2–MafG-binding sites contained TCA at N8–10 and an A after the GC box (Figure 3B). These results suggest that these nucleotides internalize an ideal sMaf-binding motif (a half-site of the MARE). To further examine the characteristics of the *in vivo* ARE, we collected motifs meeting the criteria of core ARE and categorized the motifs into four groups based on the number of variant nucleotides in N8–10 against TCA (from no variant to three variant nucleotides, Figure 3D). Whereas a large fraction of the Nrf2 single binding sites did not contain any ARE motif, at least one ARE motif was found in 84% of the Nrf2–MafG-binding sites and remarkably, >70% of those sites (61% of the total Nrf2–MafG-binding sites) are AREs without any variant nucleotides (Figure 3D). The second most abundant ARE was one bearing only a single variant nucleotide substitution (Figure 3D). The major variant nucleotides were A/G at N8, A/T at N9 and T/G at N10 (frequency >10%) (Figure 3E), and these variants are reported to still permit MafG binding (24). C at N8, G at N9 and C at N10 were only minor variants (Figure 3E) that were previously reported to have lower MafG-binding affinity (24). Altogether, these results clearly demonstrate that many AREs avoid the use of unfavorable nucleotides for sMaf binding.

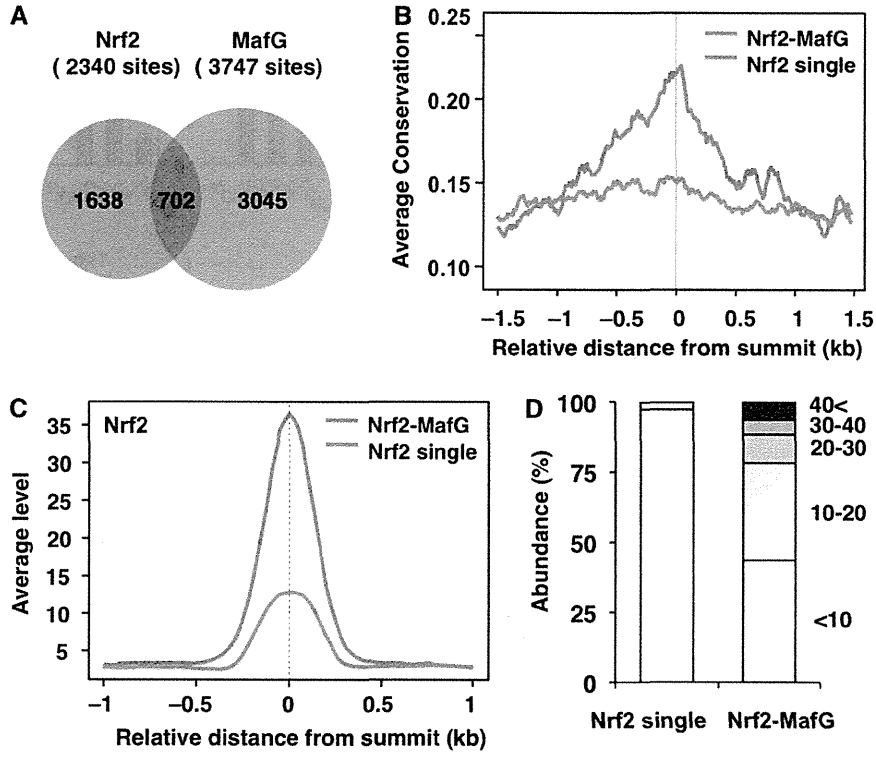

Figure 2. Characterization of TSS-proximal Nrf2- and MafG-binding sites. (**A**) Venn diagram showing the overlap between the Nrf2- and MafG-binding sites near TSS (±10 kb). (**B**) Averaged conservation profiles using PhastCons scores for Nrf2–MafG and Nrf2 single binding sites. The profiles of 3.0-kb regions centered on the peak summit are shown. (**C**) Average profiles of the Nrf2 ChIP-seq signal at the Nrf2–MafG and Nrf2 single binding sites near TSS. The profiles of 2.0-kb regions centered on the peak summit are shown. (**D**) Distribution of the fold-enrichment values of Nrf2 in the Nrf2–MafG and Nrf2 single binding sites. Classification of the fold-enrichment value is as indicated.

The functional ARE is found in part of the Nrf2–MafG-binding sites

Previous studies have suggested the importance of proximal sequences upstream of the ARE (Figure 3A; the so-called 'TMA motif', where M is A or C), and this extended ARE motif has been proposed to be the biologically functional ARE (35–37). To determine the significance of the TMA-containing ARE in the global regulation of Nrf2 target genes identified *in vivo*, we analyzed the prevalence of AREs that possess the TMA motif. We found that only ~9% of AREs found at the Nrf2–MafG-binding sites contain the TMA motif (Figure 3F). Interestingly, the enrichment of Nrf2 was higher at AREs with the TMA motif than without the TMA motif (Figure 3F). The enrichment of MafG was not significantly different between AREs with or without the TMA motif (Figure 3F). Although the precise mechanism underlying these observations is not yet known, these results suggest that the TMA-containing AREs might be utilized for the regulation of a subset of Nrf2 target genes.

The majority of Nrf2 target genes are identified in the proximal regions of the Nrf2–MafG-binding sites

As SKN-1 binds to DNA as a monomer (12), it might also be possible that the Nrf2 monomer activates its target genes through the binding of single Nrf2 molecules to ARE or altered sites. To examine the contribution of the Nrf2–MafG and Nrf2 single binding sites to the regulation of Nrf2 target genes, we identified the nearest gene to each binding site. There are 1653 genes within 10 kb of the Nrf2 single binding sites and 714 genes within 10 kb of the Nrf2–MafG-binding sites, respectively (Supplementary Table S2). To examine whether the Nrf2-dependent pathways are enriched in each gene set, KEGG pathway analyses were performed. As a result, well-known Nrf2-dependent pathways, such as glutathione metabolism, xenobiotic metabolism, ABC transporters and proteasome, were significantly enriched in genes proximal to the Nrf2–MafG-binding sites but not in genes proximal to the Nrf2 single binding sites (Table 1 and Supplementary Table S3). In addition, genes related to glucose metabolism were also enriched in genes proximal to the Nrf2–MafG-binding sites (Table 1).

We also examined a set of genes that have been reported to be Nrf2 target genes or downstream genes of Nrf2 target genes in review articles (38–41) and examined whether the same genes were found in the proximal regions of the Nrf2–MafG-binding sites. Among the 66 Nrf2 target genes proximal to the ChIP-seq identified sites, 51 genes were found in the proximal regions of the Nrf2–MafG-binding sites (Supplementary Table S4). Thus, these results suggest that the majority of Nrf2 target genes in Hepa1 cells are under the regulation of the Nrf2–MafG heterodimer.

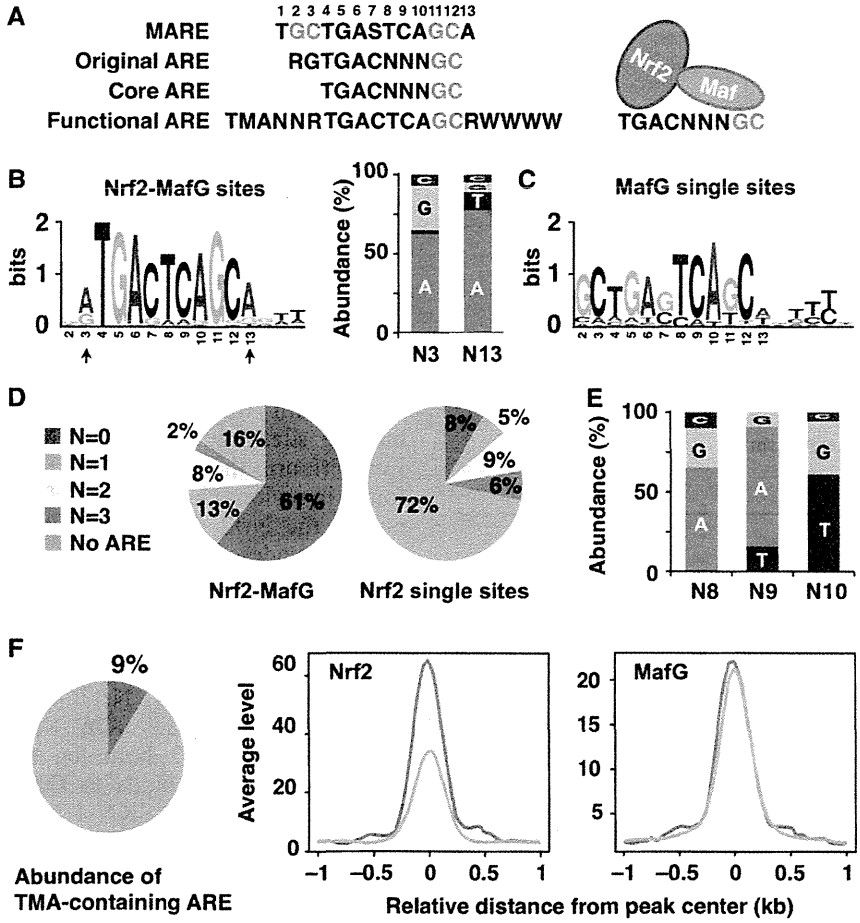

Figure 3. *In vivo* Nrf2- and MafG-binding motifs. (**A**) The consensus sequences of the MARE, original ARE, core ARE and functional ARE (S = G or C, M = A or C, R = A or G, W = A or T). GC boxes are shown in red. The left side and right side of the core ARE are shown to be recognized by Nrf2 and sMaf, respectively. (**B**, **C**) The enriched motif identified by the *de novo* motif-discovery algorithm MEME-ChIP in Nrf2–MafG-binding sites (B) and MafG single binding sites (C). The most significantly enriched motifs are shown. Nucleotide usage at N3 and N13 positions (indicated by arrows) of the enriched ARE is shown (B). (**D**) Pie charts show the percentage of classified AREs based on the number of variant nucleotides in NNN (from no variant to three variant nucleotides) in the Nrf2–MafG and Nrf2 single binding sites. The ARE motif was searched in the ± 150-nt region centered at the peaks. (**E**) Nucleotide usage at N8, N9 and N10 positions of the ARE with one variant nucleotide found in the Nrf2–MafG-binding sites. (**F**) A Pie chart shows the percentage of the TMA-containing ARE in the total core ARE found in the Nrf2–MafG-binding sites. Average profiles of Nrf2 and MafG ChIP-seq signals in the Nrf2–MafG-binding sites with (red line) or without (gray line) TMA motif. The profiles of 2.0-kb regions centered on the peak summit are shown.

DEM-inducible genes proximal to the Nrf2–MafG-binding sites

To obtain the whole picture of stress-inducible regulation mediated by Nrf2, we integrated the ChIP-seq data with the microarray data from Hepa1 cells treated with or without DEM. Among the genes proximal to the Nrf2–MafG-binding sites, 66 genes were induced by DEM (Figure 4A and C). Among the genes proximal to the Nrf2 single binding sites, only 13 genes were induced by DEM (Figure 4A and D), which suggests that the induction of the majority of Nrf2 target genes is mediated through Nrf2–MafG-binding sites. The DEM-induced genes near the Nrf2–MafG-binding sites included genes related to not only antioxidant and detoxification genes but also various cellular functions, such as chaperones, transporters and glucose metabolism (Figure 4C). Although there were DEM-repressed genes associated with the Nrf2–MafG or Nrf2 single binding sites (Figure 4B–D), their significance remains unknown. These results suggest that Nrf2–MafG heterodimers regulate genes related to cellular functions in response to stress.

NADPH-generating enzyme genes are regulated by the Nrf2–MafG heterodimer

Nrf2 regulates genes encoding NADPH-generating enzymes and contributes to NADPH-dependent redox reactions (42,43). In fact, a recent study showed that the expression of NADPH-generating enzyme genes increases in *Keap1* knockdown mice or Keap1-mutant cell lines in which Nrf2 is constitutively activated (44). However, the stress-inducibility of these groups of Nrf2 target genes has not been well documented. The present data demonstrated that NADPH-generating enzyme genes,

Table 1. KEGG pathway analysis on genes proximal to the Nrf2–MafG-binding sites

Term	*P*-value
Glutathione metabolism	1.3×10^{-12}
Metabolism of xenobiotics by cytochrome P450	8.9×10^{-9}
Drug metabolism	9.1×10^{-9}
Pyruvate metabolism	2.7×10^{-4}
Glycolysis/gluconeogenesis	0.002
ABC transporters	0.003
Pentose and glucuronate interconversions	0.005
Acute myeloid leukemia	0.010
Proteasome	0.014
Starch and sucrose metabolism	0.017
Ascorbate and aldarate metabolism	0.024
Tryptophan metabolism	0.026
Lysosome	0.029
Porphyrin and chlorophyll metabolism	0.037
Chronic myeloid leukemia	0.042
Glycerolipid metabolism	0.048

isocitrate dehydrogenase 1 (NADP+) soluble (*Idh1*), phosphogluconate dehydrogenase (*Pgd*) and glucose-6-phosphate dehydrogenase X-linked (*G6pdx*), are proximal to the Nrf2–MafG-binding sites and inducible in response to DEM (Figure 4C), which prompted us to scrutinize these reports further. A knockdown experiment using siRNA targeting Nrf2 showed that DEM induced not only *Nqo1* but also *Idh1*, *Pgd* and *G6pdx* in an Nrf2-dependent manner (Figure 5A). In addition, we confirmed that induction of *Pgd* and *G6pdx* gene expression was abolished in *F0G0K0* MEFs, which lack all three sMaf proteins (Figure 5A). *Idh1* expression was the same in MEFs of either genotype (Figure 5A), suggesting that *Idh1* gene regulation differs between Hepa1 cells and MEFs. To validate Nrf2–MafG heterodimer binding to the regulatory domains of these presumptive targets, we performed ChIP–qPCR analyses. In control cells, Nrf2 was weakly recruited to the *Nqo1*, *Idh1*, *Pgd* and *G6pdx* gene loci but not to the negative control locus, the *Txs* gene (Figure 5B). In response to DEM, Nrf2 was strongly recruited to the *Idh1*, *Pgd* and *G6pdx* loci as compared to the *Nqo1* locus (Figure 5B). In the same manner, MafG was recruited to the *Nqo1*, *Idh1*, *Pgd* and *G6pdx* gene regulatory regions in response to DEM (Figure 5B).

To obtain conclusive evidence that the Nrf2–MafG heterodimers recruited to these AREs actually participate in the transcriptional activation, we examined cofactor recruitment and histone modifications at these loci. A previous report showed that Nrf2 contains two transactivation domains, both of which interact with the coactivator CREB-binding protein (CBP) (45). We found that CBP was recruited to the regulatory regions of *Nqo1*, *Idh1*, *Pgd* and *G6pdx* moderately in control cells and more markedly in response to DEM (Figure 5B). Histone modifications reflective of transcriptional activation, such as acetylation of histone H3, H4 and H3K9, also increased in the Nrf2–MafG-binding sites and/or its flanking regions in response to DEM treatment (Figure 6). Taken together, these results demonstrated that *Idh1*, *Pgd and G6pdx* are authentic stress-inducible genes regulated by Nrf2–MafG heterodimers.

DISCUSSION

Multiple lines of evidence support the contention that Nrf2 requires sMaf proteins as an indispensable partner to bind to AREs and to activate target genes (26,46). To further substantiate this model, we identified Nrf2- and MafG-binding sites on a genome-wide scale. Compared to sites occupied by Nrf2 alone, many sites co-occupied by Nrf2 and MafG show high ChIP enrichment and are located in conserved genomic regions among species. The ARE motif was highly enriched in the Nrf2–MafG-binding sites but not in the Nrf2 single binding sites. Furthermore, the majority of the Nrf2 target genes were found in regions close to the Nrf2–MafG-binding sites but not to the Nrf2 single binding sites. Thus, the present study provides another line of convincing evidence that Nrf2–sMaf heterodimers regulate a battery of cytoprotective genes through AREs.

The Nrf2-binding sites proximal to typical Nrf2 target genes were largely overlapping with the MafG-binding sites, suggesting that Nrf2 forms heterodimers with sMafs in most cases. On the other hand, in the nematode, the Nrf2 homolog SKN-1 lacks a leucine zipper domain and binds to DNA as a monomer (12). Regardless, Nrf2 and SKN-1 both coordinately regulate a battery of cytoprotective genes. Considering these facts, we considered the possibility that Nrf2 became capable of completely changing its DNA-binding mode from monomer to heterodimer binding during the course of molecular evolution by obtaining a leucine zipper domain. While the ChIP-seq studies reported here demonstrated (weak) enrichment of Nrf2 lacking a sMaf partner, this study cannot distinguish between the possibilities that the Nrf2 monomer regulates a small fraction of target genes or that Nrf2 binds (weakly) to a subset of sites with a partner molecule that differs from the sMafs. Nonetheless, we assume that such regulation is unlikely because most of the Nrf2 single binding sites were less conserved among species and not strongly enriched in the ChIP selection (Figure 2). Furthermore, Nrf2 does not have a domain corresponding to the SKN-1 homeodomain arm, which is required for SKN-1 monomer DNA binding (10,12). Thus, these findings, together with previous biochemical and genetic evidence, strongly suggest that the Nrf2–sMaf heterodimer is the predominant complex that binds to the ARE.

The motif analyses strongly suggests that a large number of AREs found in the Nrf2–MafG-binding sites are heterodimer-oriented because: (i) many of these AREs were not MARE-like motifs that have the bilateral GC boxes that are required for strong sMaf homodimer binding and (ii) the most enriched nucleotides at the 5′-flanking end of the ARE (A and G) are known to reduce sMaf binding (24). In contrast, the MARE-like motif was enriched at the MafG-alone-binding sites (Figure 3C), which suggests that the sMaf homodimer binds to these sites to repress transcription (see

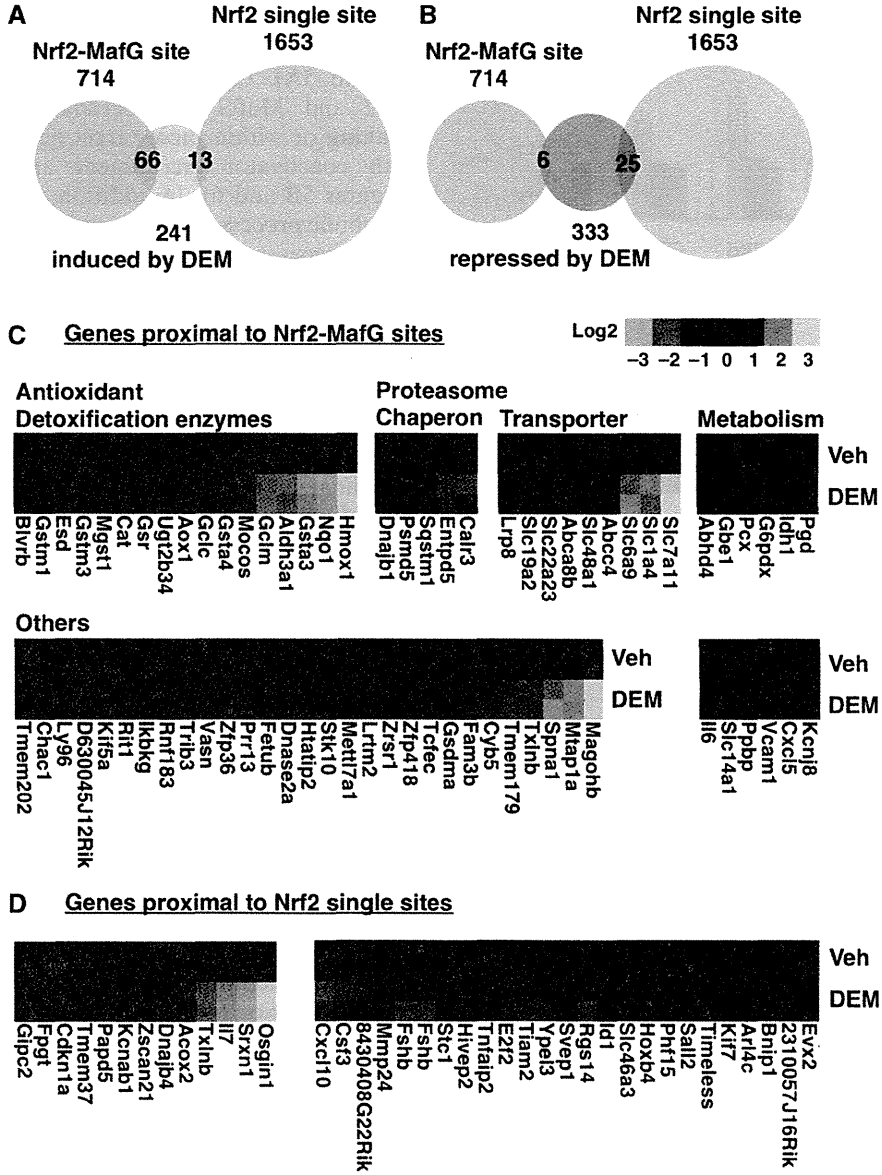

Figure 4. DEM-inducible genes proximal to Nrf2–MafG and Nrf2 single binding sites. Microarray analysis was performed with RNA isolated from DEM- or DMSO-treated Hepa1 cells for 6 h in duplicate. (**A**) Venn diagram showing the overlap of genes induced by DEM (≥1.5-fold change) and genes proximal to Nrf2–MafG or Nrf2 single binding sites. (**B**) Venn diagram showing the overlap of genes repressed by DEM (≥1.5-fold change) and genes proximal to the Nrf2–MafG or Nrf2 single binding sites. (**C**, **D**) Heat map of differentially expressed genes proximal to the Nrf2–MafG-binding sites (C) or Nrf2 single binding sites (D). DEM-induced genes proximal to Nrf2–MafG-binding sites are categorized into functional groups: antioxidant and detoxification enzymes, proteasome and chaperone, transporter, metabolism and others. The colors of the heat map reflect the $\log_{(2)}$-fold-change values relative to the mean expression level of each gene in the DMSO-treated (Veh) Hepa1 cells. The gene symbols used here are consistent with those used in the Mouse Genome Informatics database.

introduction). Although the functional significance of the sMaf homodimer needs to be examined, these results strongly suggest that Nrf2–sMaf heterodimers and sMaf homodimers are differentially utilized in different transcriptional contexts.

Whereas the core ARE sequence has been defined as TGACNNNGC, the present study clearly revealed that there exists preferential nucleotide usage at N8–10: in >60% of the enriched AREs, the N8–10 sequence is TCA (Figure 3D). These AREs contain a perfectly matched MARE half site, suggesting that the majority of these AREs possess an ideal sMaf-binding motif. We further examined the variability at N8–10 and found C, G, C to be rare nucleotides at these positions, each of which are reported to have lower MafG-binding affinity (Figure 3E) (24). Thus, the core ARE motif can be re-defined as TGACDHDGC (IUPAC code, D; not C, H; not G), giving us another distinguishing characteristic for bioinformatically identifying functional AREs.

It has been suggested that Nrf2 regulates NADPH-generating enzyme genes (42,43). We demonstrated that NADPH-generating enzyme genes, *Idh1*, *Pgd* and

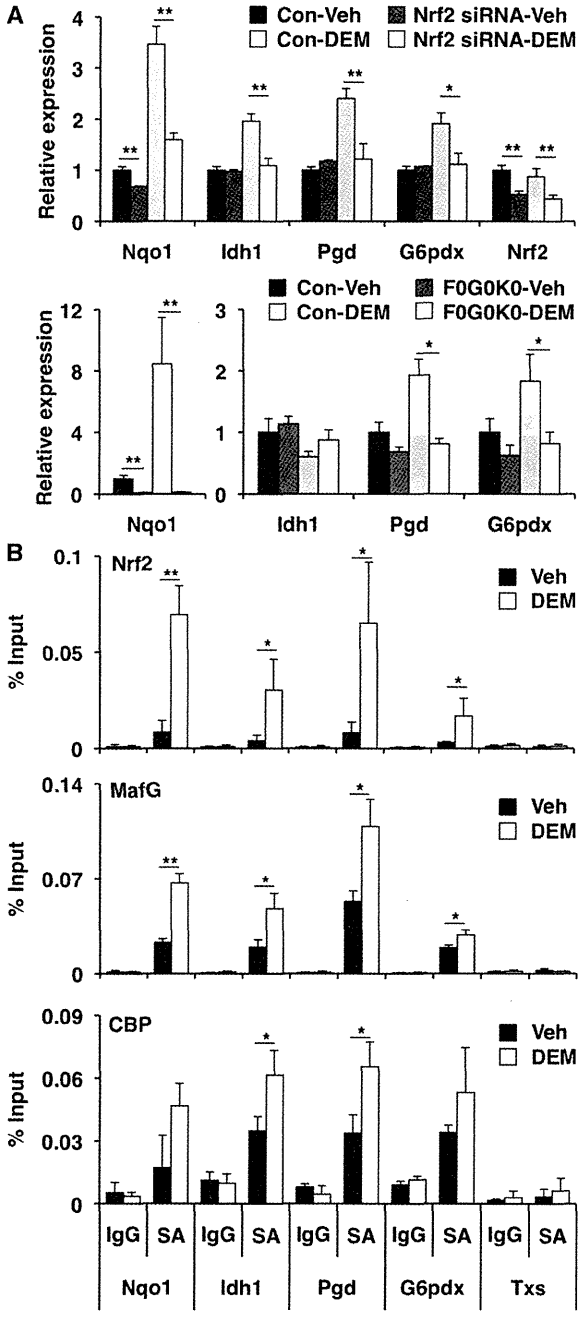

Figure 5. Nrf2–MafG heterodimer regulates the expression of NADPH-generating enzyme genes in response to DEM. (**A**) Nrf2 knockdown and sMaf deficiency impaired DEM-mediated induction of NADPH-generating enzyme gene expression. Hepa1 cells transfected with Nrf2 siRNA or control (Con) siRNA were treated with DEM or DMSO (Veh) for 6 h ($n = 3$). *F0G0K0* and control (Con) MEFs were treated with DEM or DMSO (Veh) for 12 h ($n = 4$). The mRNA expression was detected by qPCR. The data represent the mean ± SD with *P*-values derived from ANOVA with the Bonferroni *post hoc* test: $*P < 0.05$, $**P < 0.01$. (**B**) The ChIP-qPCR analyses performed with chromatin extracts from Hepa1 cells treated with 100-μM DEM or DMSO (Veh) for 4 h using specific antibodies (SA) for Nrf2, MafG or CBP. Normal IgG was used as a negative control. The amount of immunoprecipitated DNA was analyzed by qPCR with primers flanking the ARE motif in the Nrf2–MafG-binding sites in the *Nqo1*, *Idh1*, *Pgd* and *G6pdx* genomic regions. The *Txs* genomic region was used as a negative control. The data represent the mean ± SD ($n = 3$) with *P*-values from Student's unpaired *t*-test: $*P < 0.05$, $**P < 0.01$.

G6pdx, are proximal to Nrf2–MafG-binding sites and are induced by DEM in an Nrf2-dependent manner (Figures 4C and 5A). ChIP–qPCR analysis clearly showed that Nrf2 and MafG are recruited to regulatory regions flanking or within these target genes, which is coincident with coactivator recruitment and histone acetylation (Figures 5B and 6). In addition, genes related to various metabolic processes were found to be possible Nrf2–MafG target genes and may contribute to redox homeostasis. For instance, pyruvate carboxylase (Pcx), a key enzyme that catalyzes the conversion of pyruvate to oxaloacetate in mitochondria, is reported to contribute to NADPH generation by promoting the pyruvate–malate shuttle for NADPH production and the pyruvate–citrate shuttle for NADH–NADPH conversion (47). Transporter genes for amino acids for glutathione synthesis appear to be coordinately regulated by the Nrf2–sMaf heterodimer. In addition to the cysteine transporter Slc7a11 that is a well-known Nrf2 target gene (48), the cysteine transporter Slc1a4 and the glycine transporter Slc6a9 were identified here as candidate Nrf2–MafG target genes. Thus, Nrf2–sMaf heterodimers may also regulate these metabolic enzymes and transporter genes to support cellular redox homeostasis.

In addition to antioxidant and xenobiotic metabolizing functions, it is suggested that Nrf2 contributes to the regulation of cell proliferation. ChIP-seq analyses of Nrf2-binding sites identified by Malhotra *et al.* suggested that Nrf2 regulates several cell cycle-related genes (49). While not directly evaluated in the present study, our ChIP-seq data also suggest the possible contribution of Nrf2 to the regulation of cell proliferation (see Supplementary Data). The reducing power supplied by NADPH generating enzymes is also critical for efficient cell proliferation (44). Therefore, we assume that Nrf2 can be regarded as a multifunctional regulator of cell growth and survival.

In conclusion, the data shown here provide a genome-wide analysis of Nrf2 and MafG chromatin occupancy, which facilitates the examination of transcriptional mechanisms. We redefined Nrf2–MafG *cis*-regulatory elements based on their binding to sites *in vivo* and found that the Nrf2–MafG heterodimer regulates metabolic cellular functions as well as antioxidant and detoxification defense. Although we found a number of MafG-binding sites that were not associated with Nrf2 binding, it remains to be determined how MafG interacts at these sites. It is possible that sMafs bind to these sites as homodimers, acting as negative regulators and/or as heterodimers with CNC factors other than Nrf2 to activate transcription. The genome-wide binding profiles of other CNC factors will provide a comprehensive picture of the evolutionarily developed gene regulatory system mediated by CNC-sMaf factors.

SUPPLEMENTARY DATA

Supplementary Data are available at NAR Online: Supplementary Tables 1–4.

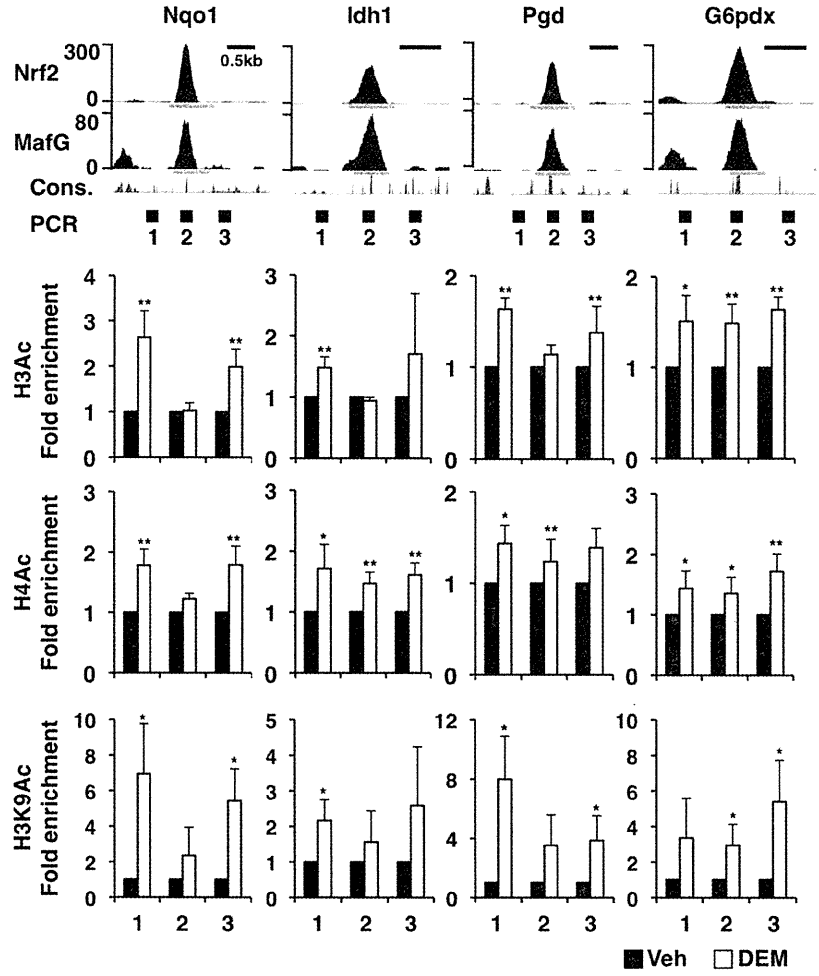

Figure 6. Stress-inducible histone acetylation at Nrf2–MafG-binding sites. ChIP-seq peak profiles surrounding the *Nqo1*, *Idh1*, *Pgd* and *G6pdx* genomic loci are shown as UCSC genome browser shots. The genomic conservation (Cons) and PCR primer positions are indicated. ChIP–qPCR analyses were performed under the same condition in Figure 5B using anti-H3Ac, anti-H4Ac or anti-H3K9Ac antibodies. The amount of immunoprecipitated DNA was analyzed by qPCR with primers flanking the ARE motif in the Nrf2–MafG-binding sites and nearly ± 500 bp of this motif in the *Nqo1*, *Idh1*, *Pgd* and *G6pdx* genomic regions. The data represent the mean ± SD ($n = 3$) with *P*-values from Student's unpaired *t*-test: $*P < 0.05$, $**P < 0.01$. Fold enrichment for DEM treatment relative to DMSO (Veh).

ACKNOWLEDGEMENTS

The authors thank Miyuki Tsuda for her help in ChIP-seq analysis and the Biomedical Research Core of Tohoku University Graduate School of Medicine for technical support.

FUNDING

The Japan Society for the Promotion of Science (JSPS) Grant-in-Aids for Creative Scientific Research [19GS0312 to M.Y.]; Young Scientist (B) [23790351 to F.K.]; Scientific Research (A) [24249015 to M.Y.]; Tohoku University Global COE program for the Conquest of Diseases with Network Medicine (to M.Y.); Mochida Pharmaceutical Co., Ltd. Y.H. is a research fellow of JSPS. Funding for open access charge: Japan Society for the Promotion of Science.

Conflict of interest statement. None declared.

REFERENCES

1. Padmanabhan,B., Tong,K., Ohta,T., Nakamura,Y., Scharlock,M., Ohtsuji,M., Kang,M., Kobayashi,A., Yokoyama,S. and Yamamoto,M. (2006) Structural basis for defects of Keap1 activity provoked by its point mutations in lung cancer. *Mol. Cell*, **21**, 689–700.
2. Sykiotis,G.P. and Bohmann,D. (2010) Stress-activated cap'n'collar transcription factors in aging and human disease. *Sci. Signal*, **3**, 1–22.
3. Itoh,K., Wakabayashi,N., Katoh,Y., Ishii,T., Igarashi,K., Engel,J.D. and Yamamoto,M. (1999) Keap1 represses nuclear activation of antioxidant responsive elements by Nrf2 through binding to the amino-terminal Neh2 domain. *Genes Dev.*, **13**, 76–86.
4. Cullinan,S.B., Gordan,J.D., Jin,J., Harper,J.W. and Diehl,J.A. (2004) The Keap1-BTB protein is an adaptor that bridges Nrf2 to a Cul3-based E3 ligase: oxidative stress sensing by a Cul3-Keap1 ligase. *Mol. Cell. Biol.*, **24**, 8477–8486.
5. Kobayashi,A., Kang,M.I., Okawa,H., Ohtsuji,M., Zenke,Y., Chiba,T., Igarashi,K. and Yamamoto,M. (2004) Oxidative stress sensor Keap1 functions as an adaptor for Cul3-based E3 ligase to regulate for proteasomal degradation of Nrf2. *Mol. Cell. Biol.*, **24**, 7130–7139.

6. Zhang,D.D., Lo,S.C., Cross,J.V., Templeton,D.J. and Hannink,M. (2004) Keap1 is a redox-regulated substrate adaptor protein for a Cul3-dependent ubiquitin ligase complex. *Mol. Cell. Biol.*, **24**, 10941–10953.
7. Itoh,K., Chiba,T., Takahashi,S., Ishii,T., Igarashi,K., Katoh,Y., Oyake,T., Hayashi,N., Satoh,K., Hatayama,I. *et al.* (1997) An Nrf2/small Maf heterodimer mediates the induction of phase II detoxifying enzyme genes through antioxidant response elements. *Biochem. Biophys. Res. Commun.*, **236**, 313–322.
8. Ramos-Gomez,M., Kwak,M.K., Dolan,P.M., Itoh,K., Yamamoto,M., Talalay,P. and Kensler,T.W. (2001) Sensitivity to carcinogenesis is increased and chemoprotective efficacy of enzyme inducers is lost in nrf2 transcription factor-deficient mice. *Proc. Natl Acad. Sci. USA*, **98**, 3410–3415.
9. Iida,K., Itoh,K., Kumagai,Y., Oyasu,R., Hattori,K., Kawai,K., Shimazui,T., Akaza,H. and Yamamoto,M. (2004) Nrf2 is essential for the chemopreventive efficacy of oltipraz against urinary bladder carcinogenesis. *Cancer Res.*, **64**, 6424–6431.
10. An,J.H. and Blackwell,T.K. (2003) SKN-1 links C. elegans mesendodermal specification to a conserved oxidative stress response. *Genes Dev.*, **17**, 1882–1893.
11. Tullet,J.M., Hertweck,M., An,J.H., Baker,J., Hwang,J.Y., Liu,S., Oliveira,R.P., Baumeister,R. and Blackwell,T.K. (2008) Direct inhibition of the longevity-promoting factor SKN-1 by insulin-like signaling in *C. elegans*. *Cell*, **132**, 1025–1038.
12. Blackwell,T.K., Bowerman,B., Priess,J.R. and Weintraub,H. (1994) Formation of a monomeric DNA binding domain by Skn-1 bZIP and homeodomain elements. *Science*, **266**, 621–628.
13. Fujiwara,K.T., Kataoka,K. and Nishizawa,M. (1993) Two new members of the maf oncogene family, mafK and mafF, encode nuclear b-Zip proteins lacking putative trans-activator domain. *Oncogene*, **8**, 2371–2380.
14. Kataoka,K., Igarashi,K., Itoh,K., Fujiwara,K.T., Noda,M., Yamamoto,M. and Nishizawa,M. (1995) Small Maf proteins heterodimerize with Fos and may act as competitive repressors of the NF-E2 transcription factor. *Mol. Cell. Biol.*, **15**, 2180–2190.
15. Itoh,K., Igarashi,K., Hayashi,N., Nishizawa,M. and Yamamoto,M. (1995) Cloning and characterization of a novel erythroid cell-derived CNC family transcription factor heterodimerizing with the small Maf family proteins. *Mol. Cell. Biol.*, **15**, 4184–4193.
16. Rushmore,T., Morton,M. and Pickett,C. (1991) The antioxidant responsive element. Activation by oxidative stress and identification of the DNA consensus sequence required for functional activity. *J. Biol. Chem.*, **266**, 11632–11639.
17. Friling,R., Bensimon,A., Tichauer,Y. and Daniel,V. (1990) Xenobiotic-inducible expression of murine glutathione S-transferase Ya subunit gene is controlled by an electrophile-responsive element. *Proc. Natl Acad. Sci. USA*, **87**, 6258–6262.
18. Motohashi,H., Katsuoka,F., Miyoshi,C., Uchimura,Y., Saitoh,H., Francastel,C., Engel,J.D. and Yamamoto,M. (2006) MafG sumoylation is required for active transcriptional repression. *Mol. Cell. Biol.*, **26**, 4652–4663.
19. Motohashi,H., O'Connor,T., Katsuoka,F., Engel,J. and Yamamoto,M. (2002) Integration and diversity of the regulatory network composed of Maf and CNC families of transcription factors. *Gene*, **294**, 1–12.
20. Mignotte,V., Eleouet,J.F., Raich,N. and Romeo,P.H. (1989) Cis- and trans-acting elements involved in the regulation of the erythroid promoter of the human porphobilinogen deaminase gene. *Proc. Natl Acad. Sci. USA*, **86**, 6548–6552.
21. Venugopal,R. and Jaiswal,A. (1998) Nrf2 and Nrf1 in association with Jun proteins regulate antioxidant response element-mediated expression and coordinated induction of genes encoding detoxifying enzymes. *Oncogene*, **17**, 3145–3156.
22. He,C.H., Gong,P., Hu,B., Stewart,D., Choi,M.E., Choi,A.M. and Alam,J. (2001) Identification of activating transcription factor 4 (ATF4) as an Nrf2-interacting protein. Implication for heme oxygenase-1 gene regulation. *J. Biol. Chem.*, **276**, 20858–20865.
23. Toki,T., Itoh,J., Kitazawa,J., Arai,K., Hatakeyama,K., Akasaka,J., Igarashi,K., Nomura,N., Yokoyama,M., Yamamoto,M. *et al.* (1997) Human small Maf proteins form heterodimers with CNC family transcription factors and recognize the NF-E2 motif. *Oncogene*, **14**, 1901–1910.
24. Yamamoto,T., Kyo,M., Kamiya,T., Tanaka,T., Engel,J., Motohashi,H. and Yamamoto,M. (2006) Predictive base substitution rules that determine the binding and transcriptional specificity of Maf recognition elements. *Genes Cells*, **11**, 575–591.
25. Kurokawa,H., Motohashi,H., Sueno,S., Kimura,M., Takagawa,H., Kanno,Y., Yamamoto,M. and Tanaka,T. (2009) Structural basis of alternative DNA recognition by Maf transcription factors. *Mol. Cell. Biol.*, **29**, 6232–6244.
26. Katsuoka,F., Motohashi,H., Ishii,T., Aburatani,H., Engel,J.D. and Yamamoto,M. (2005) Genetic evidence that small Maf proteins are essential for the activation of antioxidant response element-dependent genes. *Mol. Cell. Biol.*, **25**, 8044–8051.
27. Shang,Y., Hu,X., DiRenzo,J., Lazar,M.A. and Brown,M. (2000) Cofactor dynamics and sufficiency in estrogen receptor-regulated transcription. *Cell*, **103**, 843–852.
28. Zhang,Y., Liu,T., Meyer,C.A., Eeckhoute,J., Johnson,D.S., Bernstein,B.E., Nusbaum,C., Myers,R.M., Brown,M., Li,W. *et al.* (2008) Model-based analysis of ChIP-Seq (MACS). *Genome Biol.*, **9**, R137.
29. Machanick,P. and Bailey,T.L. (2011) MEME-ChIP: motif analysis of large DNA datasets. *Bioinformatics*, **27**, 1696–1697.
30. Liu,T., Ortiz,J.A., Taing,L., Meyer,C.A., Lee,B., Zhang,Y., Shin,H., Wong,S.S., Ma,J., Lei,Y. *et al.* (2011) Cistrome: an integrative platform for transcriptional regulation studies. *Genome Biol.*, **12**, R83.
31. Siepel,A., Bejerano,G., Pedersen,J.S., Hinrichs,A.S., Hou,M., Rosenbloom,K., Clawson,H., Spieth,J., Hillier,L.W., Richards,S. *et al.* (2005) Evolutionarily conserved elements in vertebrate,insect,worm,and yeast genomes. *Genome Res.*, **15**, 1034–1050.
32. Ji,X., Li,W., Song,J., Wei,L. and Liu,X.S. (2006) CEAS: cis-regulatory element annotation system. *Nucleic Acids Res.*, **34**, W551–W554.
33. Dignam,J.D., Lebovitz,R.M. and Roeder,R.G. (1983) Accurate transcription initiation by RNA polymerase II in a soluble extract from isolated mammalian nuclei. *Nucleic Acids Res.*, **11**, 1475–1489.
34. Lau,A., Tian,W., Whitman,S.A. and Zhang,D.D. (2012) The predicted molecular weight of Nrf2: it is what it is not. *Antioxid Redox Signal*, July 30 (doi:10.1089/ars.2012.4754: epub ahead of print).
35. Wasserman,W.W. and Fahl,W.E. (1997) Functional antioxidant responsive elements. *Proc. Natl Acad. Sci. USA*, **94**, 5361–5366.
36. Nioi,P., McMahon,M., Itoh,K., Yamamoto,M. and Hayes,J. (2003) Identification of a novel Nrf2-regulated antioxidant response element (ARE) in the mouse NAD(P)H:quinone oxidoreductase 1 gene: reassessment of the ARE consensus sequence. *Biochem. J.*, **374**, 337–348.
37. Katsuoka,F., Motohashi,H., Engel,J. and Yamamoto,M. (2005) Nrf2 transcriptionally activates the mafG gene through an antioxidant response element. *J. Biol. Chem.*, **280**, 4483–4490.
38. Kensler,T.W., Wakabayashi,N. and Biswal,S. (2007) Cell survival responses to environmental stresses via the Keap1-Nrf2-ARE pathway. *Annu. Rev. Pharmacol. Toxicol.*, **47**, 89–116.
39. Cho,H.Y. and Kleeberger,S.R. (2010) Nrf2 protects against airway disorders. *Toxicol. Appl. Pharmacol.*, **244**, 43–56.
40. Hayes,J.D., McMahon,M., Chowdhry,S. and Dinkova-Kostova,A.T. (2010) Cancer chemoprevention mechanisms mediated through the Keap1-Nrf2 pathway. *Antioxid. Redox Signal.*, **13**, 1713–1748.
41. Itoh,K., Mimura,J. and Yamamoto,M. (2010) Discovery of the negative regulator of Nrf2,Keap1: a historical overview. *Antioxid. Redox Signal.*, **13**, 1665–1678.
42. Wu,K.C., Cui,J.Y. and Klaassen,C.D. (2011) Beneficial role of Nrf2 in regulating NADPH generation and consumption. *Toxicol. Sci.*, **123**, 590–600.
43. Thimmulappa,R., Mai,K., Srisuma,S., Kensler,T., Yamamoto,M. and Biswal,S. (2002) Identification of Nrf2-regulated genes induced by the chemopreventive agent sulforaphane by oligonucleotide microarray. *Cancer Res.*, **62**, 5196–5203.
44. Mitsuishi,Y., Taguchi,K., Kawatani,Y., Shibata,T., Nukiwa,T., Aburatani,H., Yamamoto,M. and Motohashi,H. (2012) Nrf2

redirects glucose and glutamine into anabolic pathways in metabolic reprogramming. *Cancer Cell*, **22**, 66–79.
45. Katoh,Y., Itoh,K., Yoshida,E., Miyagishi,M., Fukamizu,A. and Yamamoto,M. (2001) Two domains of Nrf2 cooperatively bind CBP, a CREB binding protein, and synergistically activate transcription. *Genes Cells*, **6**, 857–868.
46. Motohashi,H., Katsuoka,F., Engel,J.D. and Yamamoto,M. (2004) Small Maf proteins serve as transcriptional cofactors for keratinocyte differentiation in the Keap1-Nrf2 regulatory pathway. *Proc. Natl Acad. Sci. USA*, **101**, 6379–6384.
47. Jitrapakdee,S., Vidal-Puig,A. and Wallace,J.C. (2006) Anaplerotic roles of pyruvate carboxylase in mammalian tissues. *Cell. Mol. Life Sci.*, **63**, 843–854.
48. Sasaki,H., Sato,H., Kuriyama-Matsumura,K., Sato,K., Maebara,K., Wang,H., Tamba,M., Itoh,K., Yamamoto,M. and Bannai,S. (2002) Electrophile response element-mediated induction of the cystine/glutamate exchange transporter gene expression. *J. Biol. Chem.*, **277**, 44765–44771.
49. Malhotra,D., Portales-Casamar,E., Singh,A., Srivastava,S., Arenillas,D., Happel,C., Shyr,C., Wakabayashi,N., Kensler,T.W., Wasserman,W.W. *et al.* (2010) Global mapping of binding sites for Nrf2 identifies novel targets in cell survival response through ChIP-Seq profiling and network analysis. *Nucleic Acids Res.*, **38**, 5718–5734.